USG Image Segmentation for Breast Cancer Detection Using the Active Contour Method

Herman Bedi Agtriadi
School of Computer Science, BINUS University, Institut Teknologi PLN Jakarta, Indonesia
herman.agtriadi@binus.ac.id (corresponding author)

Edi Abdurachman
School of Computer Science, Binus University Jakarta, Indonesia
edia@binus.ac.id

Sani Muhammad Isa
School of Computer Science, Binus University Jakarta, Indonesia
sisa@binus.edu

Boy Subirosa Sabarguna
School of Computer Science, Binus University Jakarta, Indonesia
sabar014guna@yahoo.co.id

Received: 24 March 2026 | Revised: 5 May 2026 and 13 May 2026 | Accepted: 15 May 2026

 DOI: https://doi.org/10.48084/etasr.18899

ABSTRACT

Breast cancer is one of the leading causes of cancer-related mortality among women. In Indonesia, it accounts for 16% of all cancer cases and 22.9% of invasive cancers in women. Ultrasonography (USG) is commonly used for breast imaging; however, its effectiveness is often limited by speckle noise, low contrast, and intensity inhomogeneity, which hinder accurate tumor segmentation. Therefore, this study aims to propose an effective segmentation framework for breast ultrasound images by integrating image enhancement and segmentation techniques. The proposed method combines Contrast Limited Adaptive Histogram Equalization (CLAHE) and contrast stretching for image enhancement, followed by Active Contour segmentation using the Chan–Vese model to accurately delineate tumor boundaries. CLAHE improves local contrast while controlling noise amplification, and contrast stretching enhances global intensity distribution to increase lesion–background separability. Experiments were conducted on 20 breast ultrasound images consisting of benign and malignant cases. The segmentation performance was evaluated using Receiver Operating Characteristic (ROC) analysis. The results show that for benign cases, the method achieved an accuracy of 92.35%, sensitivity of 80.5%, and specificity of 93.41%, whereas for malignant cases, it achieved an accuracy of 73.9%, sensitivity of 57.83%, and specificity of 73.49%. These findings indicate that the proposed approach is effective in improving segmentation performance and boundary detection in breast ultrasound images, although performance on malignant cases remains relatively lower.

Keywords-breast cancer; segmentation; Active Contour; Receiver Operating Characteristic (ROC); MATLAB

I. INTRODUCTION

Based on data from the Globocan Observatory 2020 of the International Agency for Research on Cancer (IARC), breast cancer is the most common cancer in the world. It is the most common cancer in women, with an estimated 2.26 million new cancer cases diagnosed (11.7% of all cancers). In terms of causes of cancer deaths worldwide, breast cancer ranks fourth with 684,996 (6.9% of all cancers) deaths [1].

Since its introduction by Dr. Cushman Haagensen in the 1950s, Breast Self-Examination (BSE) has been the subject of much controversy. Haagensen recommended that women perform BSE every 2 months. The main goal is to detect breast tumors at an early stage to reduce the number of patients diagnosed with large, inoperable cancers. At that time, the BSE technique was recognized by the National Cancer Institute and the American Cancer Society (ACS). Still, the recommended approach was later changed. Women are now encouraged to perform BSE once a month, one week after the start of their period [2, 3].

Ultrasound has become an essential tool in breast imaging. Breast ultrasound was first introduced in the 1950s using radar

techniques adapted from the US Navy. In the following decades, ultrasound in breast imaging was mainly used to distinguish cysts from solid masses. This is clinically important because simple breast cysts are a benign finding and do not require further treatment. However, most solid breast lesions remain unidentified and require biopsy because ultrasound is not specific enough to distinguish between benign and malignant breast tumors [4, 5].

Based on the description above, this study proposes an image processing system employing preprocessing and segmentation stages to address the noise problem in breast cancer digital images. Preprocessing is a technique that increases the contrast value of an image, whereas segmentation is the process of separating objects in an image based on certain characteristics to determine the boundaries of ultrasound image objects.

To overcome these challenges, Contrast Limited Adaptive Histogram Equalization (CLAHE) is selected to enhance local contrast without over-amplifying noise, whereas contrast stretching is employed to emphasize object boundaries by expanding the global intensity dynamic range. Furthermore, the Active Contour method (specifically the Chan–Vese model) is implemented due to its robustness in handling medical images characterized by high speckle noise and indistinct boundaries through the minimization of curve energy.

This method is widely used in medical image analysis because of its ability to detect object boundaries even when the edges are weak or poorly defined. By minimizing an energy function associated with the evolving curve, the model can adapt to the shapes of objects within the image, making it suitable for ultrasound images that often contain speckle noise and low contrast between tissues.

In addition, the integration of preprocessing techniques with the Active Contour segmentation method is expected to improve the accuracy and stability of tumor boundary detection in breast ultrasound images. The enhanced image quality produced during preprocessing helps the segmentation algorithm identify meaningful structures more effectively. Consequently, this approach can support more reliable image analysis, which may contribute to assisting medical professionals in the early detection and evaluation of breast abnormalities.

II. METHODOOGY

Figure 1 illustrates the proposed framework for implementing the application flow, starting with image acquisition, preprocessing, and segmentation. The Active Contour method is used to obtain segmentation results. Then, the data are recorded, and the final step is Receiver Operating Characteristic (ROC) validation to obtain the accuracy, sensitivity, and specificity of the segmentation results [6].

The workflow shown in Figure 1 follows a standard medical image processing pipeline comprising image acquisition, preprocessing, segmentation, and performance evaluation. Such a structured pipeline is commonly adopted in breast ultrasound image analysis to ensure robustness against noise and image-quality variability, particularly when contour-based segmentation methods are employed [7, 8].

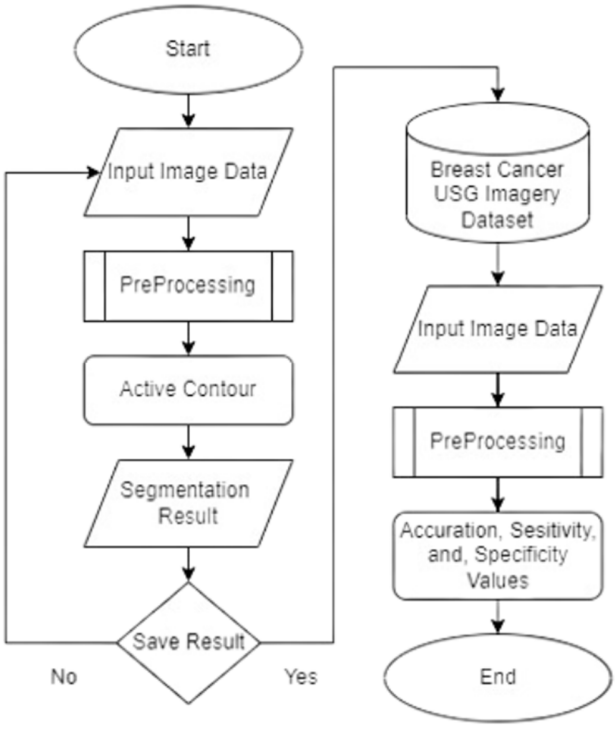

Fig. 1. Research diagram.

A. *Preprocessing*

Preprocessing is a series of transformations applied to the original images to improve image quality and make statistical analysis more reproducible and comparable. However, for breast cancer ultrasound, there is no standard preprocessing format, and the format may vary depending on the conditions [9]. Preprocessing consists of several sub-processes, namely:

- Grayscale: This stage converts a color image (RGB) into a single-channel intensity image so that the analysis process becomes simpler and more efficient. Color information is removed, whereas the main structures such as shape, texture, and edges are retained, making subsequent processing easier.
- CLAHE: CLAHE is used to enhance image contrast locally by dividing the image into several small sections (tiles), then performing histogram equalization on each section. This method is equipped with a clip limit to prevent excessive contrast enhancement so that noise is not also amplified, resulting in an image that remains balanced between detail enhancement and visual stability.
- Contrast stretching: This stage aims to expand the range of pixel intensities so that the value distribution becomes more optimal. By mapping the minimum and maximum intensity values to a new range, the difference between objects and the background becomes clearer, and details such as edges and textures can appear sharper.

Various advanced preprocessing strategies have been shown to significantly affect segmentation performance in breast ultrasound images. Hybrid approaches that combine noise-reduction filters with contrast enhancement and texture analysis help discriminate tumor edges from noisy backgrounds, thereby improving subsequent contour delineation and model robustness [10, 11].

1) Grayscale

Grayscale is the process of converting a color RGB image into a single-channel intensity image. The image has a size of $N \times M$ pixels, varying intensities represented numerically as a matrix of N rows and M columns [12]. Each RGB image consists of three channels; therefore, its representation is written as $N \times M \times 3$. The resulting grayscale image contains values ranging from 0 to 255. It is obtained by evaluating each of the R, G, and B components using the following equation:

$$\text{Grayscale}(X,Y) = 0.2989\,R + 0.587\,G + 0.114\,B \quad (1)$$

where (X, Y) denotes the pixel coordinates in the image matrix where the grayscale conversion is applied. For example, for a 5×5 image, X and Y range from (0,0) to (4,4).

Grayscale conversion is widely used in medical image processing to reduce computational complexity and stabilize intensity-based segmentation by transforming multi-channel images into a single intensity representation [13].

2) Contrast Limited Adaptive Histogram Equalization

CLAHE is a generalization of Adaptive Histogram Equalization (AHE) and improves local contrast in images [5]. CLAHE operates on small regions of the image, called tiles. After grayscale conversion, CLAHE is applied.

The probability of occurrence of intensity level r_k is defined as:

$$PR(r_k) = \frac{n_k}{M \cdot N},\ k = 0,1,2,\ldots,L-1 \quad (2)$$

where n_k is the number of pixels with intensity level r_k, and $M \cdot N$ represents the total number of pixels in the image.

The cumulative distribution function is then used to map the input intensity values to the enhanced output image. A histogram equalization mapping can be expressed as:

$$K_0 = \text{round}\left(\frac{C_i \cdot (2^k - 1)}{w \cdot h}\right) \quad (3)$$

where:

- C_i is the cumulative distribution function of the intensity level,
- round is the rounding function to the nearest integer,
- K_0 is the output intensity after equalization,
- w and h are the image width and height, respectively.

Recent studies indicate that CLAHE effectively enhances local contrast in ultrasound images while limiting excessive noise amplification. This makes the method suitable for improving lesion visibility before segmentation, particularly in low-contrast breast ultrasound images [14].

3) Contrast Stretching

Contrast stretching is a simple method for improving image contrast by stretching the intensity levels [9]. It transforms an original image (e.g., X) into a new intensity range Y. It is computed as:

$$Y(n1,n2) = 255 \cdot \frac{X(n1,n2) - Xmin}{Xmax - Xmin} \quad (4)$$

where:

- $(n1, n2)$ is the pixel position in the image matrix,
- Y is the new intensity value,
- X is the original intensity value,
- Xmax is the maximum intensity value in the image,
- Xmin is the minimum intensity value in the image.

Contrast stretching expands the dynamic range of pixel intensities, making subtle boundary information more distinguishable. When combined with histogram-based enhancement methods, this technique has been shown to improve segmentation accuracy in ultrasound imaging [15].

B. Active Contour

Active Contour is a segmentation method based on energy minimization, in which a deformable curve evolves to detect object boundaries by exploiting image properties. The curve dynamically adapts to edges or structures within the image.

Active Contour models have been extended in recent research by incorporating self-attention mechanisms and hybrid refinements to improve boundary detection in noisy ultrasound images, addressing limitations of classical energy-based formulations [16].

Active Contour is an iterative segmentation technique that evolves an initial contour toward object boundaries by minimizing an energy function. Region-based Active Contour models are particularly suitable for ultrasound images because they are less dependent on gradient information and more robust to noise [17].

The Chan–Vese model, proposed by Tony F. Chan, is a region-based Active Contour approach. It improves upon edge-based models by not relying on image gradients; instead, it is based on the Mumford–Shah functional and level-set formulation for image segmentation. In this model, contour initialization can be placed anywhere in the image, and the evolution process will adaptively converge to the object boundaries regardless of the initial position.

The segmentation process begins with contour initialization, after which the contour iteratively expands or contracts to delineate object boundaries. The number of iterations determines the extent of contour evolution and influences segmentation refinement. In this study, the parameters used include the Chan–Vese model and contraction bias [18].

Contraction bias controls the tendency of the contour to expand or shrink during evolution. Proper tuning of this

parameter is essential to avoid over-segmentation or under-segmentation, especially in noisy ultrasound images [19].

C. Initialize Regions Using Polygon

This initialization step determines the Region of Interest (ROI) in the image for the Active Contour process. The initialization process uses the polygon technique. A polygon is a geometric shape consisting of more than two points connected by line segments [20]. In this study, polygons are used to define the initial contour region in the image. Initialization scenarios were performed using 3-point and 4-point polygons, both inside and outside the object.

Initialization plays a critical role in Active Contour evolution. Improper initialization may lead to contour leakage or convergence to incorrect boundaries. Several studies have emphasized that the initial contour position significantly affects segmentation accuracy and convergence speed [21].

Figure 2 illustrates the manual initialization process used to define the starting region for the Active Contour evolution. Figure 2(a) presents a 3-point polygon example, where three strategic points are selected around the lesion to form a triangular boundary. Figure 2(b) demonstrates a 4-point polygon example, providing a more refined initial shape that closely follows the tumor morphology. This initialization step is crucial because the Active Contour (Chan–Vese) model relies on these user-defined vertices to define the initial contour, which is then iteratively expanded or contracted to fit the precise boundaries of the breast lesion.

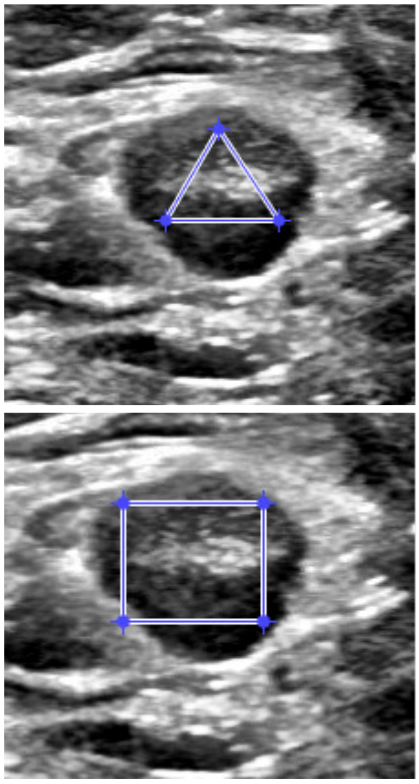

Fig. 2. Manual initialization process: (a) 3-point polygon example, (b) 4-point polygon example.

D. Initialization of Iterations

This process determines how many iterations will be performed during the Active Contour process [22]. Determining the required number of iterations is crucial for achieving optimal results. Three iteration scenarios were evaluated: 50, 100, and 300 iterations.

In the iteration initialization stage of breast ultrasound image segmentation using the Active Contour method, determining the number of iterations is a key factor because the curve deformation process is performed gradually until it reaches the desired object boundary.

At 50 iterations, the curve is generally still in the adjustment stage and may not fully follow the object contour, resulting in less stable segmentation. At 100 iterations, the curve begins to approach the object boundary more accurately, providing a balance between computational speed and segmentation quality.

At 300 iterations, the results are generally smoother and more detailed because the curve undergoes a longer convergence process, but this comes at the cost of increased computation time and a higher risk of over-segmentation if not properly controlled.

The number of iterations determines how long the contour evolves during the segmentation process [18]. Increasing the number of iterations generally improves boundary convergence until an optimal point is reached, after which additional iterations yield minimal improvement while increasing computational cost [23].

E. Dataset Description

The dataset used in this study is the Breast Ultrasound Images Dataset (BUSI), a publicly available dataset containing 780 breast ultrasound images categorized into three classes: normal, benign, and malignant. The dataset also includes corresponding ground truth masks to support segmentation and evaluation. The BUSI dataset is publicly available at [24] and further discussed in [25].

F. Implementation Details

The proposed segmentation framework was implemented and tested using MATLAB (R2015a). The implementation includes the CLAHE method, contrast stretching, and the Active Contour model. A Graphical User Interface (GUI) was also developed in MATLAB (R2015a) to facilitate image processing and visualization of the segmentation results.

G. Receiver Operating Characteristic Analysis

ROC analysis is used to evaluate the performance of a classification or diagnostic system. Sensitivity and specificity are fundamental measures of diagnostic accuracy; however, these measures depend on the threshold used to define positive and negative test results. As the threshold changes, the sensitivity and specificity also change. The ROC curve plots sensitivity against the false-positive rate for all possible threshold values, enabling the assessment of diagnostic performance and the identification of an optimal operating point.

ROC analysis is widely used to evaluate the performance of medical image segmentation methods. By analyzing sensitivity, specificity, and accuracy, ROC-based evaluation provides an objective assessment of how well the segmentation algorithm distinguishes between lesion and non-lesion regions in breast ultrasound images [26].

From the four values true positive (TP), true negative (TN), false positive (FP), and false negative (FN), accuracy, sensitivity, and specificity can be calculated as follows:

$$\text{Accuracy} = \frac{\text{TP+TN}}{\text{TP+TN+FP+FN}} \quad (5)$$

$$\text{Sensitivity} = \frac{\text{TP}}{\text{TP+FN}} \quad (6)$$

$$\text{Specificity} = \frac{\text{TN}}{\text{TN+FP}} \quad (7)$$

The regions representing TP, TN, FP, and FN are illustrated in Figure 3.

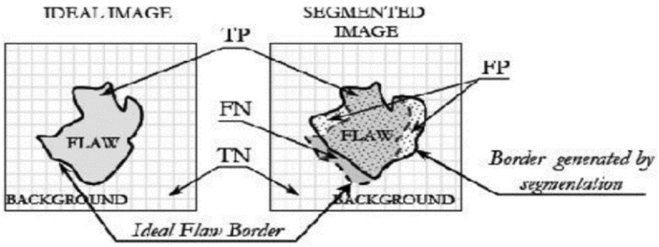

Fig. 3. Comparison between manual and program-generated segmentation.

Figure 3 presents a visual comparison between the manual segmentation performed by a medical expert (ground truth) and the automated segmentation results generated by the proposed program.

The left image displays the manual delineation, which serves as the reference standard for evaluating accuracy. The right image shows the segmentation result produced by the Active Contour algorithm after the application of CLAHE and contrast stretching [27].

The comparison demonstrates that the program-generated segmentation closely aligns with the manually delineated boundary, indicating that the integration of contrast enhancement techniques with the Chan–Vese model effectively addresses the challenges of indistinct edges and speckle noise. This visual consistency suggests good performance in preserving the actual morphology of the breast lesion.

III. RESULTS AND DISCUSSION

A. Segmentation Results

The segmentation results for benign breast cancer cases exhibit well-defined and smooth boundary characteristics. Example results of the data testing are shown in Table I.

In Table II, the results of ultrasound image segmentation for malignant breast cancer cases show irregular and less-defined boundary characteristics.

TABLE I. RESULTS OF TESTING ULTRASOUND IMAGE DATA FOR BENIGN BREAST CANCER

No	Original image	Preprocessing result image and initialization region	Active Contour segmentation results
1	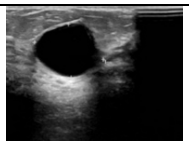 Benign 9	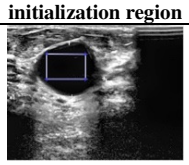	
2	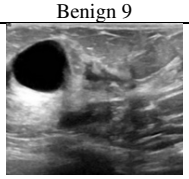 Benign 10	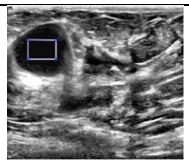	

TABLE II. RESULTS OF TESTING ULTRASOUND IMAGE DATA FOR MALIGNANT BREAST CANCER

No	Original image	Preprocessing result image and initialization region	Active Contour segmentation results
1	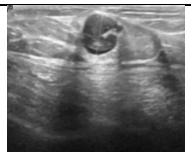 Malignant 26		
2	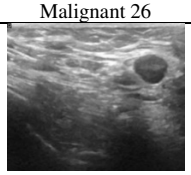 Malignant 28	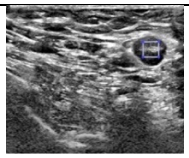	

B. Segmentation Performance Evaluation Using ROC Analysis

The segmentation results are evaluated in terms of accuracy, sensitivity, and specificity using ROC analysis. Table III presents the performance of the proposed method on benign breast cancer ultrasound images. The results show consistently high performance, with most samples achieving accuracy above 90%. For instance, Benign 15 achieved a peak accuracy of 98.56%. This indicates that well-defined lesion boundaries in benign cases allow effective convergence of the Active Contour model when combined with CLAHE and contrast stretching.

Table IV presents the results for malignant breast cancer cases, which show greater variability in performance. While some images, such as Malignant 95, maintain a high accuracy of 89.16%, others, such as Malignant 93, show a significant drop to 29.30%. This variance provides a technical insight: malignant tumors often have spiculated or irregular margins and are frequently accompanied by acoustic shadowing. In cases such as Malignant 93, the program misinterprets the posterior shadow as part of the tumor mass, leading to contour leakage. This suggests that, although the proposed method is robust, it faces challenges when dealing with complex

shadowing artifacts commonly observed in invasive breast cancer.

TABLE III. PERFORMANCE RESULTS FOR BENIGN BREAST CANCER ULTRASOUND IMAGES BASED ON ROC ANALYSIS

No	Image name	Accuracy (%)	Sensitivity (%)	Specificity (%)
1	Benign 9	86.0291	90.4485	72.947
2	Benign 10	92.1219	91.5382	92.7289
3	Benign 15	98.5626	78.4776	99.7751
4	Benign 23	88.6871	79.9293	92.3286
5	Benign 26	90.4251	89.2282	91.7837
6	Benign 34	86.0626	66.8651	91.2493
7	Benign 87	98.0667	89.7409	99.4907
8	Benign 89	92.8955	67.9957	97.0676
9	Benign 95	97.6074	76.1736	98.8767
10	Benign 99	93.129	74.6993	97.86

TABLE IV. PERFORMANCE RESULTS FOR MALIGNANT BREAST CANCER ULTRASOUND IMAGES BASED ON ROC ANALYSIS

No	Image name	Accuracy (%)	Sensitivity (%)	Specificity (%)
1	Malignant 26	88.2278	69.603	92.9365
2	Malignant 28	91.4246	68.0385	95.0614
3	Malignant 34	86.4792	67.0635	92.0522
4	Malignant 35	52.1545	60.9772	38.0308
5	Malignant 93	29.2999	38.362	16.834
6	Malignant 131	87.7747	70.3872	92.4535
7	Malignant 135	41.7923	50.1514	30.0301
8	Malignant 143	83.1192	55.1022	89.6106
9	Malignant 145	93.6432	49.3443	96.6134
10	Malignant 166	85.1166	49.2803	91.3618

Table V summarizes the average performance for both classes. The results indicate higher performance for benign cases compared with malignant cases, with accuracy, sensitivity, and specificity of 92.3587%, 80.5096%, and 93.4108%, respectively, for benign lesions, and 73.9032%, 57.8310%, and 73.4948%, respectively, for malignant lesions.

TABLE V. AVERAGE SEGMENTATION PERFORMANCE OF ACTIVE CONTOUR FOR BREAST ULTRASOUND IMAGES USING ROC ANALYSIS

No	Image name	Accuracy (%)	Sensitivity (%)	Specificity (%)
1	Benign	92.3587	80.5096	93.4108
2	Malignant	73.9032	57.8310	73.4984

This performance gap between the two categories provides several key insights. The high accuracy in benign cases indicates that the combination of CLAHE and contrast stretching successfully clarifies the well-defined boundaries typical of benign lesions, allowing the Active Contour model to converge precisely. On the other hand, the lower sensitivity in malignant cases (57.83%) reflects the inherent challenges of ultrasound imaging, such as spiculated margins and intensity inhomogeneity. In these complex cases, the algorithm occasionally struggles to distinguish between the invasive edges of a malignant tumor and the surrounding shadowed tissue.

This suggests that, although the current framework is highly effective for circumscribed masses, further optimization of the contour's internal energy is needed for handling irregular malignant morphologies.

Figure 4 illustrates the systematic stages of the proposed segmentation framework. The process begins with image acquisition, where raw breast ultrasound images are retrieved. To address the inherent low contrast and speckle noise, CLAHE is applied to enhance local features, followed by contrast stretching to widen the global intensity distribution, making the lesion more distinguishable against the background.

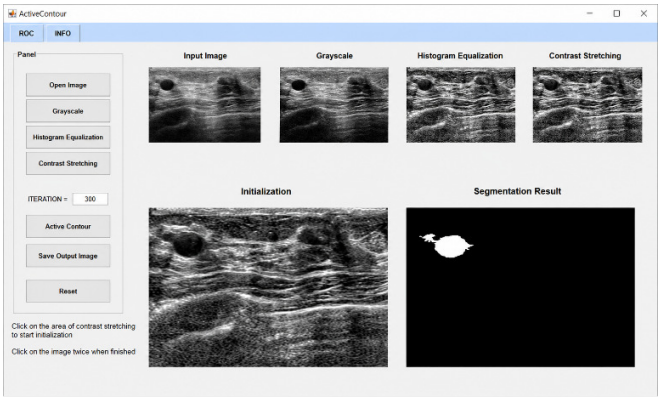

Fig. 4. Segmentation process.

Once the image is enhanced, the ROI is manually defined as a polygon around the suspected lesion. This initial contour serves as the starting point for Active Contour (Chan–Vese) evolution, in which the curve iteratively deforms to minimize the energy functional until it converges to the tumor boundary. The final stage involves extraction of the segmented region for quantitative analysis.

Figure 5 illustrates the comparison between manual segmentation (ground truth) and program-generated segmentation results [28, 29]. The left image represents the manual annotation, whereas the right image shows the output of the proposed method. The visual similarity in shape and area indicates good agreement between the automated and manual segmentations. Evaluation metrics including accuracy, sensitivity, and specificity are used to quantify this agreement [30, 31]. Higher metric values indicate better agreement between automated and reference segmentations.

Overall, these results suggest that the proposed approach performs effectively in segmenting breast ultrasound images, although further validation on more diverse datasets is required to ensure robustness.

C. Implications

In this study, 20 breast cancer images were used as the dataset, consisting of 10 benign and 10 malignant cases. As shown in Table I, benign breast cancer images exhibit well-defined, firm borders, whereas Table II shows that malignant breast cancer images are characterized by irregular and poorly defined boundaries.

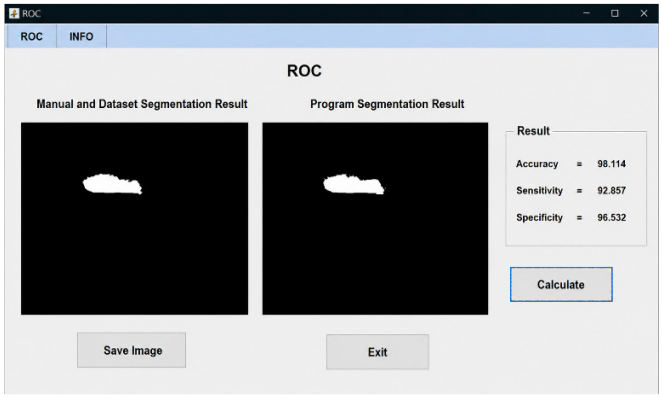

Fig. 5. ROC analysis and segmentation comparison.

The findings of this study provide significant contributions to the field of medical image processing, particularly in breast cancer diagnosis. The primary contribution is the development of a robust segmentation framework that integrates CLAHE, contrast stretching, and the Active Contour model to address the inherent limitations of Ultrasonography (USG).

First, this study demonstrates that CLAHE is effective in stabilizing local intensity variations and preventing over-amplification of speckle noise, which is a common limitation of standard histogram equalization methods. Second, contrast stretching serves as an important bridge between preprocessing and segmentation by optimizing the global intensity dynamic range, thereby improving the performance of the Active Contour energy functional.

The main implication of this study is that accurate tumor boundary detection in USG cannot rely on a single segmentation method alone. By combining contrast enhancement techniques with the Chan–Vese model, the proposed framework provides a more reliable tool for clinicians, achieving high accuracy (92.36%) in delineating benign lesions. This approach serves as a foundational step toward automated Computer-Aided Diagnosis (CAD) systems that are less sensitive to the low-contrast environment of breast ultrasound images.

IV. CONCLUSIONS

This study presents a segmentation approach for breast cancer ultrasound images using the Active Contour method. The preprocessing stage involves converting color ultrasound images into grayscale, followed by image enhancement using the Contrast Limited Adaptive Histogram Equalization (CLAHE) method and contrast stretching. These techniques are applied to improve image quality by enhancing contrast and expanding the dynamic range, thereby facilitating more accurate segmentation.

The Active Contour segmentation method demonstrates distinct characteristics in differentiating tumor types. Benign breast cancer images tend to exhibit well-defined and regular boundaries, whereas malignant cases are characterized by irregular and unclear borders. A total of 20 breast cancer ultrasound images were used in this study. The segmentation performance was evaluated using the Receiver Operating Characteristic (ROC) approach. The results indicate that the method achieved an accuracy of 92.35%, sensitivity of 80.5%, and specificity of 93.41% for benign cases, whereas for malignant cases, it achieved an accuracy of 73.9%, sensitivity of 57.83%, and specificity of 73.49%.

Overall, the results demonstrate that the Active Contour method is effective for segmenting breast cancer ultrasound images, particularly for benign tumor identification, although performance on malignant cases remains relatively lower.

DECLARATION OF COMPETING INTERESTS

The authors declare that they have no known competing financial interests or personal relationships that could have appeared to influence the work reported in this paper.

ACKNOWLEDGMENT

The authors would like to thank the LPPM of Institut Teknologi PLN for supporting and funding this research through the Research Grant Program. The contents are solely the responsibility of the author.

DATA AVAILABILITY

The dataset used in this study is the Breast Ultrasound Images Dataset (BUSI), a publicly available breast ultrasound imaging dataset containing 780 images categorized into three classes: normal, benign, and malignant. The dataset also provides corresponding ground truth masks to support image segmentation and evaluation processes. The BUSI dataset is publicly accessible through the Kaggle platform [24].

AI USE AND DECLARATION OF GENERATIVE AI USE

The authors used generative AI to improve the writing clarity of this paper. They reviewed and edited the AI-assisted content and take full responsibility for the final publication.

REFERENCES

[1] H. Sung *et al.*, "Global Cancer Statistics 2020: GLOBOCAN Estimates of Incidence and Mortality Worldwide for 36 Cancers in 185 Countries," *CA: A Cancer Journal for Clinicians*, vol. 71, no. 3, pp. 209–249, May 2021, https://doi.org/10.3322/caac.21660.

[2] S. M. Albeshan, S. Z. Hossain, M. G. Mackey, and P. C. Brennan, "Can Breast Self-examination and Clinical Breast Examination Along With Increasing Breast Awareness Facilitate Earlier Detection of Breast Cancer in Populations With Advanced Stages at Diagnosis?," *Clinical Breast Cancer*, vol. 20, no. 3, pp. 194–200, June 2020, https://doi.org/10.1016/j.clbc.2020.02.001.

[3] Kriti, J. Virmani, and R. Agarwal, "A Characterization Approach for the Review of CAD Systems Designed for Breast Tumor Classification Using B-Mode Ultrasound Images," *Archives of Computational Methods in Engineering*, vol. 29, no. 3, pp. 1485–1523, May 2022, https://doi.org/10.1007/s11831-021-09620-8.

[4] T. A. Sardjono, A. F. H. Chozin, and M. Nuh, "Semi-Automatic Image Segmentation on X-ray Image of Spine using Active Contour Method," *JAREE (Journal on Advanced Research in Electrical Engineering)*, vol. 5, no. 2, pp. 89–92, Oct. 2021, https://doi.org/10.12962/jaree.v5i2.166.

[5] R. Iacob *et al.*, "Evaluating the Role of Breast Ultrasound in Early Detection of Breast Cancer in Low- and Middle-Income Countries: A Comprehensive Narrative Review," *Bioengineering*, vol. 11, no. 3, Mar. 2024, Art. no. 262, https://doi.org/10.3390/bioengineering11030262.

[6] A. Nour and B. Boufama, "Hybrid deep learning and active contour approach for enhanced breast lesion segmentation and classification in

mammograms," *Intelligence-Based Medicine*, vol. 11, Jan. 2025, Art. no. 100224, https://doi.org/10.1016/j.ibmed.2025.100224.

[7] G. Qi, Z. Zhu, K. Li, and H. Xiao, "Advancements and Challenges in Medical Image Segmentation: A Comprehensive Survey," *Sensors and AI*, vol. 1, no. 1, pp. 3–29, Mar. 2025, https://doi.org/10.53941/sai.2025.100002.

[8] M. Biesok, J. Juszczyk, and P. Badura, "Breast tumor segmentation in ultrasound using distance-adapted fuzzy connectedness, convolutional neural network, and active contour," *Scientific Reports*, vol. 14, no. 1, Oct. 2024, Art. no. 25859, https://doi.org/10.1038/s41598-024-76308-x.

[9] A. Bunnell, K. Hung, J. A. Shepherd, and P. Sadowski, "BUSClean: Open-source software for breast ultrasound image pre-processing and knowledge extraction for medical AI," *PLOS ONE*, vol. 19, no. 12, Dec. 2024, Art. no. e0315434, https://doi.org/10.1371/journal.pone.0315434.

[10] A. Nugroho *et al.*, "Automated Ultrasound Object Segmentation Using Combinatorial Active Contour Method," *Jurnal Ilmu Komputer dan Informasi*, vol. 17, no. 2, pp. 203–218, June 2024, https://doi.org/10.21609/jiki.v17i2.1298.

[11] X. Shen, H. Ma, R. Liu, H. Li, J. He, and X. Wu, "Lesion segmentation in breast ultrasound images using the optimized marked watershed method," *BioMedical Engineering OnLine*, vol. 20, no. 1, June 2021, Art. no. 57, https://doi.org/10.1186/s12938-021-00891-7.

[12] W. El-Shafai, I. Almomani, A. Ara, and A. Alkhayer, "An optical-based encryption and authentication algorithm for color and grayscale medical images," *Multimedia Tools and Applications*, vol. 82, no. 15, pp. 23735–23770, June 2023, https://doi.org/10.1007/s11042-022-14093-3.

[13] W. Liu, N. Lv, J. Wan, L. Wang, and X. Zhou, "Pixel embedding for grayscale medical image classification," *Heliyon*, vol. 10, no. 16, Aug. 2024, Art. no. e36191, https://doi.org/10.1016/j.heliyon.2024.e36191.

[14] T. Berhe and E. Diriba, "Enhancement of Mammogram Images Using Digital Image Processing Techniques for Breast Cancer Detection," *Journal of Science, Technology and Arts Research*, vol. 13, no. 4, pp. 188–198, Dec. 2024, https://doi.org/10.20372/star.V13.i4.13.

[15] T. Wang *et al.*, "DCCE-UNet: a difference and context-aware contrast enhanced framework for ultrasound image segmentation," *BMC Medical Imaging*, vol. 25, no. 1, Nov. 2025, Art. no. 445, https://doi.org/10.1186/s12880-025-01954-0.

[16] Y. Zhao, X. Shen, J. Chen, W. Qian, L. Sang, and H. Ma, "Learning active contour models based on self-attention for breast ultrasound image segmentation," *Biomedical Signal Processing and Control*, vol. 89, Mar. 2024, Art. no. 105816, https://doi.org/10.1016/j.bspc.2023.105816.

[17] M. Shi and I. Hussain, "Improved region-based active contour segmentation through divergence and convolution techniques," *AIMS Mathematics*, vol. 10, no. 1, pp. 654–671, Jan. 2025, https://doi.org/10.3934/math.2025029.

[18] Y. Chen, P. Ge, G. Wang, G. Weng, and H. Chen, "An overview of intelligent image segmentation using active contour models," *Intelligence & Robotics*, vol. 3, no. 1, pp. 23–55, Feb. 2023, https://doi.org/10.20517/ir.2023.02.

[19] M. Tamoor and I. Younas, "Automatic segmentation of medical images using a novel Harris Hawk optimization method and an active contour model," *Journal of X-Ray Science and Technology*, vol. 29, no. 4, pp. 721–739, July 2021, https://doi.org/10.3233/XST-210879.

[20] S. A. Hussein and Q. O. Mosa, "Medical Image Segmentation with active contour and optimization Techniques: Survey," *Journal of Al-Qadisiyah for Computer Science and Mathematics*, vol. 14, no. 4, pp. 82–89, Dec. 2022, https://doi.org/10.29304/jqcm.2022.14.4.1115.

[21] Y. S. Malik, M. Tamoor, A. Naseer, A. Wali, and A. Khan, "Applying an adaptive Otsu-based initialization algorithm to optimize active contour models for skin lesion segmentation," *Journal of X-Ray Science and Technology*, vol. 30, no. 6, pp. 1169–1184, Nov. 2022, https://doi.org/10.3233/XST-221245.

[22] M. Mahmuddin, Z. N. M. Alqattan, N. H. Harun, and H. Harun, "An improved active contour model for food image segmentation," *International Journal of Innovative Research and Scientific Studies*, vol. 8, no. 4, pp. 2672–2683, July 2025, https://doi.org/10.53894/ijirss.v8i4.8535.

[23] M. A. Al-Ebrahim, "Spike-Based Attention Mechanisms for Enhanced Medical Image Segmentation," *Engineering, Technology & Applied Science Research*, vol. 15, no. 5, pp. 28273–28285, Oct. 2025, https://doi.org/10.48084/etasr.13407.

[24] "Breast Ultrasound Images Dataset." Kaggle. [Online]. Available: https://www.kaggle.com/datasets/aryashah2k/breast-ultrasound-images-dataset.

[25] W. Al-Dhabyani, M. Gomaa, H. Khaled, and A. Fahmy, "Dataset of breast ultrasound images," *Data in Brief*, vol. 28, Feb. 2020, Art. no. 104863, https://doi.org/10.1016/j.dib.2019.104863.

[26] T. Jiang *et al.*, "Deep learning-assisted diagnosis of benign and malignant parotid tumors based on ultrasound: a retrospective study," *BMC Cancer*, vol. 24, no. 1, Apr. 2024, Art. no. 510, https://doi.org/10.1186/s12885-024-12277-8.

[27] M. M. Philip *et al.*, "Comparison of semi-automatic and manual segmentation methods for tumor delineation on head and neck squamous cell carcinoma (HNSCC) positron emission tomography (PET) images," *Physics in Medicine & Biology*, vol. 69, no. 9, Apr. 2024, Art. no. 095005, https://doi.org/10.1088/1361-6560/ad37ea.

[28] S. Z. Kurdi, "Machine Learning–Based Classification Framework for Human Health Care Monitoring," *International Journal of Theoretical & Applied Computational Intelligence*, vol. 2026, pp. 1–15, Jan. 2026, https://doi.org/10.65278/IJTACI.2026.1.

[29] B. Mughal, M. Sharif, N. Muhammad, and T. Saba, "A novel classification scheme to decline the mortality rate among women due to breast tumor," *Microscopy Research and Technique*, vol. 81, no. 2, pp. 171–180, 2018, https://doi.org/10.1002/jemt.22961.

[30] B. Mughal, N. Muhammad, M. Sharif, A. Rehman, and T. Saba, "Removal of pectoral muscle based on topographic map and shape-shifting silhouette," *BMC Cancer*, vol. 18, no. 1, Aug. 2018, Art. no. 778, https://doi.org/10.1186/s12885-018-4638-5.

[31] M. Karimi *et al.*, "Feature Selection Methods in Big Medical Databases: A Comprehensive Survey," *International Journal of Theoretical & Applied Computational Intelligence*, vol. 2025, pp. 181–209, Sept. 2025, https://doi.org/10.65278/IJTACI.2025.21.